The Journal of Chemical Physics

Radical ions with nearly degenerate ground state: Correlation between the rate of spin-lattice relaxation and the structure of adiabatic potential energy surface

V. I. Borovkov, I. V. Beregovaya, L. N. Shchegoleva, P. A. Potashov, V. A. Bagryansky et al.

Citation: J. Chem. Phys. **137**, 104305 (2012); doi: 10.1063/1.4749247
View online: http://dx.doi.org/10.1063/1.4749247
View Table of Contents: http://jcp.aip.org/resource/1/JCPSA6/v137/i10
Published by the American Institute of Physics.

Radical ions with nearly degenerate ground state: Correlation between the rate of spin-lattice relaxation and the structure of adiabatic potential energy surface

V. I. Borovkov,[1,2,a)] I. V. Beregovaya,[3] L. N. Shchegoleva,[3] P. A. Potashov,[1,2] V. A. Bagryansky,[1,2] and Y. N. Molin[1]
[1]*Institute of Chemical Kinetics and Combustion of SB RAS, 3, ul. Institutskaya, 630090, Novosibirsk, Russia*
[2]*Novosibirsk State University, Novosibirsk, 630090, Russia*
[3]*N.N. Vorozhtsov Institute of Organic Chemistry, 9, pr. Ak. Lavrentyeva., Novosibirsk, 630090, Russia*

(Received 5 July 2012; accepted 17 August 2012; published online 10 September 2012)

Paramagnetic spin-lattice relaxation (SLR) in radical cations (RCs) of the cycloalkane series in liquid solution was studied and analyzed from the point of view of the correlation between the relaxation rate and the structure of the adiabatic potential energy surface (PES) of the RCs. SLR rates in the RCs formed in x-ray irradiated *n*-hexane solutions of the cycloalkanes studied were measured with the method of time-resolved magnetic field effect in the recombination fluorescence of spin-correlated radical ion pairs. Temperature and, for some cycloalkanes, magnetic field dependences of the relaxation rate were determined. It was found that the conventional Redfield theory of the paramagnetic relaxation as applied to the results on cyclohexane RC, gave a value of about 0.2 ps for the correlation time of the perturbation together with an unrealistically high value of 0.1 T in field units for the matrix element of the relaxation transition. The PES structure was obtained with the DFT quantum-chemical calculations. It was found that for all of the cycloalkanes RCs considered, including low symmetric alkyl-substituted ones, the adiabatic PESes were surfaces of pseudorotation due to avoided crossing. In the RCs studied, a correlation between the SLR rate and the calculated barrier height to the pseudorotation was revealed. For RCs with a higher relaxation rate, the apparent activation energies for the SLR were similar to the calculated heights of the barrier. To rationalize the data obtained it was assumed that the vibronic states degeneracy, which is specific for Jahn-Teller active cyclohexane RC, was approximately kept in the RCs of substituted cycloalkanes for the vibronic states with the energies above and close to the barrier height to the pseudorotation. It was proposed that the effective spin-lattice relaxation in a radical with nearly degenerate low-lying vibronic states originated from stochastic crossings of the vibronic levels that occur due to fluctuations of the interaction between the radical and the solvent. The magnitude of these fluctuations, $\sim$100 cm^{-1}, determines the upper scale of the unperturbed splitting between the vibronic states, for which the manifestation of this paramagnetic relaxation mechanism could be expected. Our estimate for the relaxation rate derived using standard Landau-Zener model of nonadiabatic transitions at the level crossing agrees with the experimental data. This paramagnetic relaxation mechanism can also be operative in paramagnetic species of other types such as linear radicals, radicals with threefold degeneracy, paramagnetic centers in crystals, etc. It looks likely that the proposed SLR mechanism can be quenched by a fast vibrational relaxation in radicals. © *2012 American Institute of Physics*. [http://dx.doi.org/10.1063/1.4749247]

I. INTRODUCTION

The energy exchange between a spin system and thermostat, i.e., the other degrees of freedom with a relatively high density of energy levels, is usually described in terms of spin-lattice (or longitudinal) relaxation. For organic radicals in solutions, the spin-lattice relaxation of unpaired electrons is determined, as a rule, by interactions of the electron spin magnetic moment with the magnetic moments of the nuclei and with the electron orbital moment.[1–3]

In solutions, the spin lattice relaxation time T_1 for organic radicals containing atoms of only the first and the second rows of the periodic table varies, as a rule, within the range of several microseconds at magnetic field strength of 0.3–1 T.[1,4] However, much shorter relaxation times have been observed in some organic radicals. The radical anions of aromatic molecules with the symmetry axis of the third or higher order were the first among them.[5] For example, for benzene radical anion, the spin-lattice relaxation time T_1 in solution is about 150 ns.[6] Much shorter spin-lattice relaxation times have been observed for C60 fullerene radical anion, down to $\sim$1 ns at room temperature.[7,8] Even more effective paramagnetic relaxation seems to be found in radical anion C70 in the solid phase ($\sim$100 ps).[9] More recently, anomalously fast

a)Author to whom correspondence should be addressed. Electronic mail: borovkov@kinetics.nsc.ru.

paramagnetic relaxation has been observed in highly symmetric radical cations (RCs) of cyclohexane and adamantane (∼10 ns).[10,11]

The interest to spin-lattice relaxation in highly symmetric radicals is inspired by the lack of success in attempts to explain the high relaxation rate by conventional mechanisms (see, e.g., Refs. 6, 10, and 12). Moreover, during the last five decades, no distinctive explanations for an effective coupling between the unpaired electron spin and other degrees of freedom in highly symmetric organic radicals have been suggested.

It is worth noting that the interest to this problem bears not only an academic character. The highly symmetric molecular objects, such as fullerenes and nanotubes, are discussed to be used as the structural units of nanodimensional devices to manipulate the state of a single electron spin (see, e.g., Refs. 13–15). In such devices, the spin state lifetime should be long enough. Therefore, it is necessary to investigate the paramagnetic relaxation mechanisms in symmetric molecular structures with an open electron shell.

The distinctive feature of the aforementioned radical ions is that their structure and spectral properties are determined by vibronic interactions, i.e., the interactions of the electrons with vibrational motion of the nuclei. When the vibronic interactions are strong enough, in accordance with the Jahn-Teller theorem,[16,17] the highly symmetric structure is not a stationary potential energy surface (PES) structure but corresponds to the conical intersection point. Adiabatic PES becomes multiwell and is formed by the structures of lowered symmetry. As an example, the minimum-energy structure of cyclohexane molecule is of D_{3d} symmetry while the PES of its radical cation ($E\times e$ Jahn-Teller problem[17]) has three minima corresponding to three energetically and geometrically equivalent structures of C_{2h} symmetry with the ^2A_g ground state and three saddle points corresponding to C_{2h} structures with the ^2B_g ground state.[18] The lowest-energy path between the minima on the PES lies away from the conical intersection point and thus avoids the recovery of the initial molecule symmetry. This type of the intramolecular motion is referred to as pseudorotation.[17,19]

More rigorously, the ground state of the Jahn-Teller active radicals is a superposition of electronic and vibrational states and may keep the degeneracy in vacuum. In condensed phase, external interactions having low symmetry typically stabilize one of the distorted nuclear configurations. Nevertheless, transitions between the distorted structures of a Jahn-Teller active radical are possible that can be observed experimentally (see, e.g., Refs. 18 and 20–22).

For the problems considered in the present work, of importance is the fact that the mentioned transitions modulate both the hyperfine interactions and the Zeeman interaction (due to the changing g-tensor components) of the unpaired electron spin. In the EPR spectra, these transitions manifest themselves already at low temperatures since barrier heights to the pseudorotation in the Jahn-Teller active radicals are often negligible (<1 kcal/mol) even in the presence of the matrix effect.[22] Undoubtedly, the modulation of electron spin interactions due to the structural transitions similar to the stochastic motion of other types contributes to the spin-lattice relaxation.[3,12] Nevertheless, as mentioned above, this contribution is insufficient for providing the observed spin-lattice relaxation rate for the highly symmetric radicals.

Another intriguing fact is that the high symmetry of the initial molecule is not of decisive importance for the fast relaxation. In particular,[10,23] radical cations of *trans*-decalin (C_{2h}) and a series of the alkyl-substituted cyclohexanes (the symmetry being not higher than C_s) exhibit unexpectedly effective paramagnetic relaxation, too. In this case, of interest are the works[24–26] demonstrating by example of the radical ions of a series of fluorobenzenes that the crossing of the electron state terms and thus, the pseudorotation, are conserved in some low-symmetric derivatives of the Jahn-Teller ions. Besides, our recent study[27] on the PESes of the RCs of low-symmetric bicyclic alkanes, *cis*- and *trans*-decalins, has shown the existence of energetically close electron states of different symmetry for these RCs as well. The adiabatic PESes of both of the RCs look like the pseudorotation surfaces but differ, in particular, in barrier heights (∼2 and ∼9 kcal/mol for the *trans*- and the *cis*-isomer, respectively). It is worth noting that the spin-lattice relaxation times also differ for these RCs by more than order of magnitude (14 ns for the *trans*- and ∼400 ns for the *cis*-isomer).[10]

The above examples suggest that the peculiarities of the adiabatic PES structure and the anomalously fast spin-lattice relaxation are tightly related to each other. The goal of this work is to look into the relationship deeper by comparing the experimental spin-lattice relaxation rates for the series of cycloalkane radical cations with the characteristics of corresponding PESes. This comparison allowed us to propose a novel mechanism of paramagnetic relaxation in the studied radicals. Preliminary results have been briefly discussed in Ref. 23.

II. METHODS

A. Approach

As previously,[10,11,23] we measured spin-lattice relaxation rate of cycloalkane radical cations using the method of time-resolved magnetic field effect (TR MFE) in the delayed fluorescence originating from the geminate recombination of spin-correlated radical ion pairs.[28] The TR MFE curve is given by the $I_B(t)/I_0(t)$ ratio between the fluorescence intensity decays registered at high ($I_B(t)$) and zero ($I_0(t)$) magnetic fields. Being determined by spin evolution of spin-correlated radical ion pairs, the TR MFE curve contains information on hyperfine coupling constants and the g-values of the radical ions as the ESR spectrum of the same radical ions does. At the same time, in contrast to the conventional ESR method, the rate of spin-lattice relaxation can be readily measured using the TR MFE curve since the long-time decay of the curve can, typically, be approximated by a simple exponent

$$\frac{I_B(t)}{I_0(t)} - 1 \approx \theta \cdot \exp\left(-\frac{t}{T_1}\right), \tag{1}$$

where $1/T_1$ is the sum of the spin-lattice relaxation rates of radicals composing the pair. The parameter θ, equal to 0.2–0.25 for the solutions studied, is introduced to take into

account that only a part of primary radical ion pairs arises as being the singlet-correlated ones.[29] Its value is actually of no essence for using Eq. (1) to obtain T_1.

B. Experimental

The geminate radical pairs including the radical cations of cycloalkanes under study were generated by pulsed x-ray irradiation of the *n*-hexane solutions of corresponding cycloalkanes at the concentration in the range of 0.01–0.1 M. As electron acceptor and luminophore, *para*-terphenyl (*p*TP) was used in concentrations of $(3 \div 10) \times 10^{-6}$ M.

The formation rates of cycloalkane radical cations and *p*TP radical anions are controlled by the diffusion of primary *n*-hexane solvent holes and excess electrons, respectively. At the concentrations used, typical times of the formation are of the order of 1 ns and 50 ns for the secondary positive and negative charge carriers, respectively. Over the time range under study (<1 μs), the *p*TP molecules take no part in the capture of the positive charge due to their low concentration. Therefore, after a few nanoseconds the delayed fluorescence observed from the irradiated solutions appears dominantly due to reaction

$$(\text{cycloalkane})^{+\bullet} + p\text{TP}^{-\bullet} \rightarrow (\text{cycloalkane}) + {}^1p\text{TP}^* \qquad (2)$$

because other possible reactions yielding the electronically excited states of the luminophore can be neglected.

The delayed fluorescence decays were recorded using a nanosecond x-ray fluorimeter[30] operating in the single photon counting regime with an optical bandpass filter (260–390 nm). The maximal magnetic field value reached approximately 1.9 T. Zero magnetic field was adjusted within 0.05 mT. To decrease the influence of instrumental drift, the fluorescence decays were registered for periods of 250 s, alternatively, with and without external magnetic field.

n-Hexane ("Fluka", 99.5%) was passed several times through a 1 m column of activated alumina and stored over sodium. Cyclohexane (cH), methylcyclohexane (Me-cH), ethylcyclohexane (Et-cH), propylcyclohexane (*n*Pr-cH), *iso*-propylcyclohexane (*i*Pr-cH), *tert*-butylcyclohexane (*t*Bu-cH), *trans*-decalin (*t*-DEC), and *cis*-decalin (*c*-DEC) were received from Aldrich and passed through a 0.5 m column of activated alumina before use. *para*-Terphenyl (98%), cyclohexane-d_{14} (99.5%), 1,1-dimethylcyclohexane (1,1-Me_2-cH, 99%), *cis*-1,2-dimethylcyclohexane (1,2-Me_2-cH, 99%), *cis*-1,4-dimethylcyclohexane (1,4-Me_2-cH, 98%) were used as received from Aldrich. The solutions were degassed by repeated freeze-pump-thaw cycles.

The spin-lattice relaxation of $p\text{TP}^{-\bullet}$ is comparatively slow[10] ($T_1 \approx 4$ μs), which provides a more reliable information on the temperature and magnetic field dependence of the paramagnetic relaxation of a RC under study as compared to our previous results[10] obtained with hexafluorobenzene as an electron acceptor. Note that excess electrons are very likely to contribute to the spin-relaxation rate negligibly before scavenging by *p*TP. So, the spin-lattice relaxation time of cycloalkane radical cations can be calculated from the parameter T_1 in Eq. (1) with a high accuracy.

C. Details of quantum-chemical calculations

The preliminary ROHF calculations (see also Ref. 27) showed that, for all the alkylcyclohexane RCs (R-cH$^{+\bullet}$) studied, the terms of lower $^2A'$ and $^2A''$ electron states of symmetric C_s conformations intersect. The crossing of the states results in a possibility of pseudorotation in the RCs.

As in Ref. 27, we used spin-unrestricted DFT B3LYP/6-31G* calculations[31] for the PES studies. For comparison, some BHHLYP/6-31G* calculations[32] were also performed. The types of the stationary PES points were determined by normal vibrations analysis. Interrelations between the points were established by the intrinsic reaction coordinate (IRC) technique. We neglected the corrections for zero-point vibration energy (ZPVE) when estimated the barrier heights, because the PESes studied are flattened in the vicinity of minima and the harmonic approximation that usually used for the Hessian calculations may result in large error. Besides, the low symmetry of most of the systems studied makes it impossible to distinguish pseudorotational vibration modes at the PES minima whereas the respective vibration frequencies are necessary for accurate determining the ZPVE correction to the barrier heights. Our estimation for cH$^{+\bullet}$ and Me-cH$^{+\bullet}$ where we could with more or less certainty distinguish the pseudorotational modes gave correction values of about -0.4 kcal/mol.

All these PES calculations were carried out by the GAMESS package.[33] To control the adequacy of results we used data on the low-temperature EPR spectra.[18,34–39] We used the GAUSSIAN 98 package[40] to locate the structures corresponding to conical intersection points at the PESes of cH$^{+\bullet}$, Me-cH$^{+\bullet}$, and Et-cH$^{+\bullet}$, and to estimate the spin-orbit coupling in these radicals. These state-average calculations were performed at the CASSCF(5,5)/6-311G* level.

III. RESULTS

A. Quantum-chemical calculations

In the present work, we have studied the adiabatic PESes of the alkylcyclohexane radical cations, for which the experimental values of the spin-lattice relaxation time vary within two orders of magnitude. Table I summarizes calculated energies of the RC stationary structures. The constants of isotropic hyperfine coupling (HFC) with ^{1}H nuclei calculated for these structures are presented in Table II along with the literature data on EPR studies in low temperature matrices. In Tables I and II as well as in the text we use the same labeling scheme for the structures relating to the symmetry properties of single-occupied molecular orbital (SOMO). The latter can be symmetric (S) or antisymmetric (A) to the symmetry plane passing through the marked carbon atom of the cyclohexane fragment (see Fig. 1). The shape of the PES for cH$^{+\bullet}$ is determined by the $(E\times e)$-Jahn-Teller effect. The highly symmetric D_{3d} (^2E_g) RC structure with the degenerate ground electron state corresponds to the conic intersection point, which, according to the ROHF data, lies about 14 kcal/mol higher than the structures with the lower C_{2h} symmetry corresponding to the PES minima. The conical intersection point is avoided along the pseudorotation

TABLE I. Relative energies (kcal/mol) for the stationary PES structures of alkyl-cyclohexane radical cations, R-cH$^{+\bullet}$, and total energies for the global minima ($E_{\min}$, a.u.).[a]

R	$E_{\min}$ (a.u.)	S(0)	A(π/3)	S(–π/3)	A(0)	S(π/3)	A(–π/3)
			B3LYP				
H	−235.35738	**0**	*0.5*	**0**	*0.5*	**0**	*0.5*
Me	−274.65201	*2.9*	...	**0**	*1.5*	**0**	...
Et[b]	−313.93994	**0**	*2.2*	**0.9**	*2.2*	**0.3**	*0.5*
Et[c]	−313.93779	**1.4**	*2.4*	**1.7**	*2.4*	**1.7**	*3.9*
*n*Pr[b,d]	−353.22955	...	*4.2*	**3.5**	*4.0*	...	**0**
*i*Pr	−353.23042	**0**	*4.0*	**3.8**	*5.0*	**3.8**	*4.0*
*t*Bu	−392.52216	**0**	...	...	*9.9*	...	...
1,4-Me$_2$	−313.93753	**1.9**	*2.0*	**0**	*0.2*	**0**	*2.0*
1,1-Me$_2$	−313.94273	*4.6*	*4.8*	**0**	*2.3*	**0**	*2.0*
1,2-Me$_2$	−313.94394	**0**	*4.8*	**4.6**	*6.3*	**4.3**	*4.4*
			BHHLYP				
Me	−274.662425	*6.6*	...	**0**	*4.0*	**0**	...
Et[b]	−313.951977	**1.1**	*4.0*	**0.7**	*4.1*	**0**	*2.6*
*n*Pr[b,d]	−353.242050	**0.8**	*4.7*	**1.4**	*4.8*	**0**	*1.5*
1,1-Me$_2$	−313.958001	*7.4*	*8.1*	**0**	*4.8*	**0**	*8.1*

[a]PES minima are marked by the bold font, the italic one stands for saddle points, and the underlined values correspond to the barrier to pseudorotation defined as $E_B = E_{\max} - E_{\min}$.
[b]Staggered conformation (rotation angle of the alkyl fragment $\beta \approx \pm 60^\circ$).
[c]Eclipsed conformation ($\beta = 180^\circ$). Note that the global PES minimum lies at $\beta \approx \pm 60^\circ$.
[d]*n*-Propyl group has all-*trans* conformation.

coordinate with a smooth change in the electron state. The pseudorotational trough includes six stationary structures of C_{2h} symmetry (see Fig. 1 presenting the PES scheme and SOMOs of the stationary structures). The extended C_{2h} (^2B_g) structures (S(φ) in the Fig. 1) correspond to the PES minima while the compressed structures, C_{2h} (^2A_g) or A(φ), correspond to transition states (TS). SOMOs of the minimum energy structures, as well as the TS SOMOs, differ by a rotation of the local coordinate system by an angle φ multiple to $\pi/3$, which is reflected in the structure labeling. Note that the additional decrease in symmetry up to C_s, observed earlier in UHF/STO-3G and 4-31G calculations,[38] disappeared on going to B3LYP (see also Ref. 41), but remains in the BHHLYP calculations (see notes to Table II). Note that according to ESR measurements,[18] in matrices at 4 K the $C_{2h}(^2A_g)$ structure of cyclohexane radical cation is stabilized. As the temperature increases to 140 K, the spectrum corresponds to the dynamic averaging of HFC between the $C_{2h}(^2B_g)$ and $C_{2h}(^2A_g)$ structures.

The calculation results show that for alkylcyclohexanes with the equatorial substituent $CH_3(CH_2)_n$ ($n \geq 1$) the most favorable conformation is the staggered one where the α-C–C bond is twisted relative to the axial H atom by the angle $\beta \approx 60^\circ$. Independently of conformation, the higher occupied MOs of the R-cH molecules represent the perturbed components of the degenerate cyclohexane e_g MO.

Figure 2 illustrates this using Et-cH$^{+\bullet}$ as an example. As for cH$^{+\bullet}$, extended S(0) and compressed A(0) stationary structures are present at the PESes of all studied R-cH$^{+\bullet}$, including those having no symmetry elements. The S(0) and A(0) structures correspond to electron ionization from ψ_S and ψ_A components of the e_g MO, respectively (Fig. 1), i.e., these

TABLE II. Experimental (matrix isolation) and calculated HFC constants[a] a_H for alkyl-cyclohexane radical cations, R-cH$^{+\bullet}$.

		B3LYP/6-31G*		BHHLYP/6-31G*	
R	Experiment	a_H/G	Structure	a_H/G	Structure
H	85 (2H), 34 (2H), 14 (2H)[b] 84 (2H), 39 (2H), 13 (2H)[c]	102 (2H), 14 (4H)	**S(0)**	110(2H), 14 (4H)	**S(0)**
Me	78, 70[d] 81,77, 35, 12[e] 74(2H), 34[f]	85, 76, 39, 9	**S(±π/3)**[h]	68, 60, 41, 8.5	**S(±π/3)**
Et	69 (2H)[f] 76, 62, 16[e]	82, 68, 11, 8	**S(+π/3)**	67, 58, 7.6, 7.4	**S(+π/3)**
*n*Pr	67 (2H),17[f] 72, 56, 16[e]	74, 62, 19, 7.7	**S(+π/3)**[i]	67, 54, 8.2, 7.3	**S(+π/3)**
*i*Pr	31 (2H), 18[f]	35, 33, 18	**S(0)**		
*t*Bu	31 (3H)[f]	30, 29, 27	**S(0)**		
1,1-Me$_2$	61 (2H), 29 (2H)[f]	67, 55, 33, 28	**S(±π/3)**	57, 47, 33, 31	**S(±π/3)**
1,2-Me$_2$	59 (2H), 31 (2H)[g]	57, 55, 34, 34	**S(0)**	...	...
1,4-Me$_2$	53(4H)[g]	86, 82, 18; 61(2H), 57(2H)	**S(±π/3)** **A(0)**[j]	...	...

[a]If the number of equivalent nuclei exceeds unity, it is indicated in parentheses.
[b]Reference 18, three pair of equivalent protons are probably the result of a matrix effect.
[c]Reference 38.
[d]Reference 36.
[e]Reference 35.
[f]References 34 and 37.
[g]Reference 39.
[h]Local minimum.
[i]Non-stationary structure.
[j]This TS lies only 0.2 kcal/mol higher than the global minimum **(S±π/3)** (see text).

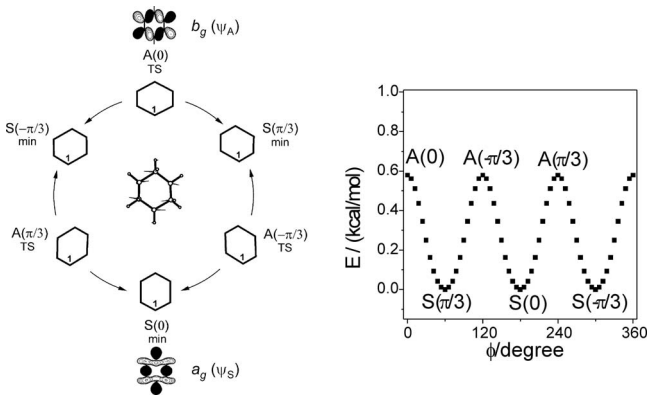

FIG. 1. Pseudorotation scheme, SOMO images and designations of stationary structures for cyclohexane radical cation (to the left). Pseudorotation coordinate is shown at the center of the scheme. The plot to the right shows the PES cross-sections along the pseudorotation trough (B3LYP). Since the trough has a cyclic shape, it is convenient to use the angle ϕ ($0 < \phi < 360^\circ$) as the pseudorotation coordinate.

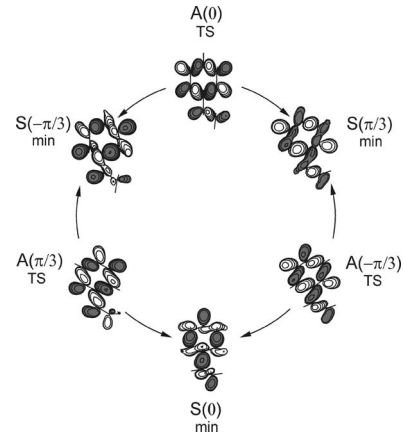

FIG. 2. Pseudorotation scheme and SOMOs of stationary structures for staggered conformation of ethylcyclohexane radical cation. The ethyl fragment is attached to the cyclohexane ring at atom 1 as labeled in Fig. 1.

have different ground electron states and are related by pseudorotation. For the above R-cH$^{+\bullet}$, the pseudorotation trough includes all the structures depicted in Fig. 1 but not all of them are stationary for every particular RC. The number of stationary structures and the pseudorotation barrier height E_B, determined as energy difference between the trough stationary structures of minimum and maximum energy, vary in the RC series under study (Table I, Fig. 3).

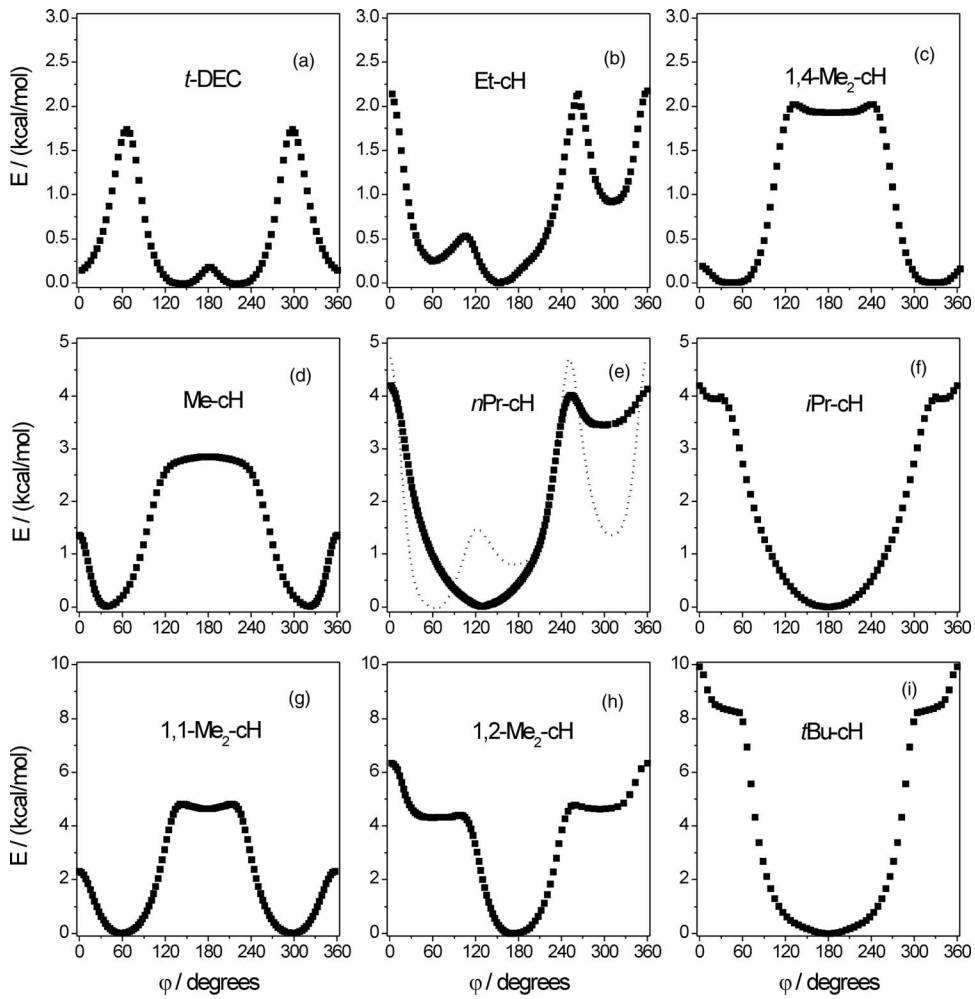

FIG. 3. The PES sections along the pseudorotation trough (B3LYP) for the cycloalkane RCs studied. Here the angle ϕ is the pseudorotation coordinate, $\phi = 0$ corresponds to A(0) structures. The dashed line added to the plot e) denotes BHHLYP calculations for Pr-cH$^{+\bullet}$. Note that the plots show the different vertical scale.

Below we describe the distinctive features of RCs with different substituents.

1. Methylcyclohexane radical cation

Introducing a methyl group, so as other alkyl substituents, causes a substantial distortion of the cyclohexane ring. The pseudorotation trough includes four stationary structures (see Fig. 3(d)). The PES minima correspond to the asymmetric mirror structures S($\pm\pi/3$) in which one of the ring bonds at the substituted position is elongated by almost 0.3 Å. These minima are divided by the two nonequivalent TSes, S(0), and A(0). The HFC constants a_H calculated at the PES minimum are in fair agreement with the experimental ones measured at 4 K (Table II).

As for the results of energy calculation, comparison with EPR data on the spectral exchange between two equivalent Me-d_3-cH$^{+\bullet}$ structures over the temperature range 4–173 K show that the calculated value of the height of the smaller barrier (~1.5 kcal/mol) is much higher as compared to the estimation[36,37] (~0.2 kcal/mol) obtained from ESR experiment in the CF_3-*c*-C_6F_{11} matrix.

2. Ethylcyclohexane radical cation

The PES structure of the Et-cH$^{+\bullet}$ is more complex because of the feasible conformation isomerism. According to calculation results, the staggered conformation of the RC is energetically preferable. There are two equivalent pseudorotation cycles with $\beta \approx \pm 60^\circ$, both including six stationary structures (Fig. 2). The structures with the eclipsed conformation ($\beta \approx 180^\circ$) are higher in their energy and they also form the pseudorotation cycle of six structures. The minima of these three cycles are related by TSes for the ethyl group rotation. The height of the barriers between the minima at $\beta \approx \pm 60^\circ$ and $\beta \approx 180^\circ$ is 4.3–5.0 kcal/mol.

Note that for a neutral molecule the staggered conformation is also more advantageous by ~2 kcal/mol. Therefore, after ionization, the equivalent staggered RC conformations are mainly populated, and the set of available stationary structures is determined by cycles with $\beta \approx \pm 60^\circ$ (see Fig. 3(b)). The height of the pseudorotation barrier within each cycle is about 2 kcal/mol which is comparable with that of the barriers for transition between minima in various cycles.

The pseudorotation scheme and the SOMO of stationary structures are similar for Et-cH$^{+\bullet}$ (Fig. 2) and cH$^{+\bullet}$ (Fig. 1) except for the fact that in the staggered Et-cH$^{+\bullet}$ conformation, the structures S($\pi/3$) and S($-\pi/3$), as well as the A($\pi/3$) and A($-\pi/3$) ones are energetically nonequivalent. According to the B3LYP calculations, a global PES minimum corresponds to the S(0) structure. However, the HFC constants calculated for this structure do not agree with EPR data. In fair agreement with experiments are the a_H values calculated for the S($\pi/3$) structure whose energy is by 0.3 kcal/mol higher than that of S(0) (Fig. 3(b)). Taking into account the closeness of the energies, the above disagreement can be assigned either to the effect of the matrix, which mainly stabilizes S($\pi/3$) structure, or to the calculation errors resulting in the overestimated S(0) structure stability.

3. n-Propylcyclohexane radical cation

According to the B3LYP calculations, the *n*Pr substituent causes a dramatic change in PES as compared with the aforementioned Me and Et substituents. In this case, there no minima corresponding to the S($\pm\pi/3$) and S(0) structures, and the global PES minimum corresponds to the A($-\pi/3$) structure (Fig. 3(e)). However, neither of the stationary structures offers a satisfactory explanation of the experimental HFC constants.[35] Calculations of various conformation *n*Pr-cH$^{+\bullet}$ isomers have also failed. Therefore, we have performed additional calculations of the PES for *n*Pr-cH$^{+\bullet}$, Me-cH$^{+\bullet}$, Et-cH$^{+\bullet}$, and 1,1-Me_2-cH$^{+\bullet}$ using the BHHLYP functional. The calculation results are also given in Tables I and II.

For the Me-cH$^{+\bullet}$, Et-cH$^{+\bullet}$, and 1,1-Me_2-cH$^{+\bullet}$, the BHHLYP results are in qualitative agreement with the B3LYP ones except for changing the relative positions of the energetically close structures S($\pi/3$) and S(0) of Et-cH$^{+\bullet}$ that is in accord with the EPR data. At the same time, BHHLYP provides a worse description of HFC constants and twice as high barriers although the ratios between the pseudorotation barrier heights for these RCs are qualitatively the same for both of the functionals. In particular, for Me-cH$^{+\bullet}$, we can consider the calculated height of the barrier determined by the A(0) structure (4 kcal/mol) as greatly overestimated in the light of the above data on the high rate of spectral exchange in Me-cH$^{+\bullet}$ at low temperatures.[36]

Unlike the Me-cH$^{+\bullet}$ and Et-cH$^{+\bullet}$ RCs, for *n*Pr-cH$^{+\bullet}$, the use of the BHHLYP functional changes qualitatively the form of the calculated PES (Tables I and II, Fig. 3(e)). In this case, PES structure becomes similar to that of Et-cH$^{+\bullet}$: the pseudorotation trough consists of six stationary structures, and the global minimum corresponds to the S($\pi/3$) structure. The calculated HFC constants are now in qualitative agreement with the experimental ones. In the B3LYP calculations, the S($\pi/3$) structure is non-stationary but can be found, however, from IRC calculations of the path from A(0) to A($-\pi/3$) by following the changes in geometry and SOMO. The a_H constants calculated for this non-stationary structure reproduce well the experimental values (Table II).

Comparing the calculated results for Et-cH$^{+\bullet}$ and *n*Pr-cH$^{+\bullet}$ with two different functionals, we can conclude that B3LYP leads to erroneous results in estimating the relative energies of stationary structures for RCs with long linear alkyl substituents. A systematic error of this functional has already been observed in the calculations on the *n*-alkane molecules.[42] According to Table II, for all other RCs studied in this work, the results of B3LYP calculations are in fair agreement with the experiment.

For our further discussion it is important that, according to the BHHLYP data, the height of the pseudorotation barrier E_B for *n*Pr-cH$^{+\bullet}$ should be between the values for Et-cH$^{+\bullet}$ and Me-cH$^{+\bullet}$. Assuming that for the two last RCs, the results of B3LYP calculations are accurate enough, then for *n*Pr-cH$^{+\bullet}$, the pseudorotation barrier height should be about 2.5 kcal/mol.

As for Et-cH$^{+\bullet}$, in the case of *n*Pr-cH$^{+\bullet}$, there are three PES sheets corresponding to the staggered ($\beta \approx \pm 60^\circ$) and the eclipsed ($\beta \approx 180^\circ$) conformations and thus, three

pseudorotation cycles. By the data of BHHLYP calculations, the pseudorotation barrier heights within these cycles are almost the same and amount to about 4 kcal/mol. Transitions between the PES sheets are followed by the change in the orientation of a propyl fragment with the overcoming of the barriers whose height is also about 4 kcal/mol. Note that the actual barrier height for the transitions between the pseudorotation surfaces is likely to be much lower and the transition rate may be comparatively high.

4. iso-Propylcyclohexane and tert-butylcyclohexane radical cations

According to the B3LYP data for both the RCs, the minimum energy corresponds to the S(0) structures. The HFC constants calculated for these structures agree well with the experimental ones (Table II). The branched alkyl substituents draw significantly the SOMO density away from the cyclohexane ring. The increasing perturbation of the levels, which are degenerate in cH radical cation, leads to the increase in the barrier height to pseudorotation. The maximum energy in both RC corresponds to the A(0) structures. For the *i*Pr-cH$^{+\bullet}$, the barrier height is about 5 kcal/mol (Fig. 3(f)). The pseudorotation trough is formed by six stationary structures again, but the depth of local minima is relatively small. In *t*Bu-cH$^{+\bullet}$, the pseudorotation barrier increases almost to 10 kcal/mol, and the local minima disappear (Fig. 3(i)). There are only two stationary PES points at the pseudorotation trough, one of them corresponds to the minimum and the other to the TS structure.

5. Bialkylcyclohexane radical cations

We have also considered the RCs of three bialkylcyclohexanes 1,1-Me$_2$-cH$^{+\bullet}$, 1,2-Me$_2$-cH$^{+\bullet}$, and 1,4-Me$_2$-cH$^{+\bullet}$. Their PESes also hold the shape of pseudorotation surface. The structures corresponding to the global PES minima, S($\pm\pi/3$) for 1,1-Me$_2$-cH$^{+\bullet}$ and S(0) for 1,2-Me$_2$-cH$^{+\bullet}$, reproduce well the EPR data (Table II). In the case of 1,4-Me$_2$-cH$^{+\bullet}$, the HFC constants, calculated by the B3LYP method for the structures of minimum energy S($\pm\pi/3$), disagree with the experimental ones. At the same time, the HFC constants, calculated for the A(0) structure, whose energy is by 0.2 kcal/mol higher, are close to the experimental ones. This may be assigned to a relative stabilization of the A(0) structure due to the interaction with the matrix. However, the calculations errors cannot be excluded as well.

As in the case of Me-cH$^{+\bullet}$, the calculated height of the smaller barrier for 1,1-Me$_2$–cH$^{+\bullet}$ is overestimated as compared with the EPR data.[36]

B. Experiment

Figure 4 shows the experimental curves of the time-resolved magnetic field effect at B = 1 T obtained for the 0.03 M solutions of cycloalkanes in *n*-hexane. In the (cycloalkane)$^{+\bullet}$/*p*TP$^{-\bullet}$ pairs, the rate of the dynamic singlet-triplet evolution determined mainly by substantial HFCs in the RC is higher than that of the spin-lattice relaxation in all the cases. Therefore, the TR MFE curves first increases rapidly and finally decreases approximately exponentially with time. As mentioned above, the decay time gives almost directly the time T_1 for the RC involved. When the relaxation time T_1 in a radical ion pair is not too short and HFCs are not very large (e.g., for the *t*Bu-cH solution), a characteristic peak caused by the dynamic spin evolution due to the HFCs is observed on the TR MFE curve.

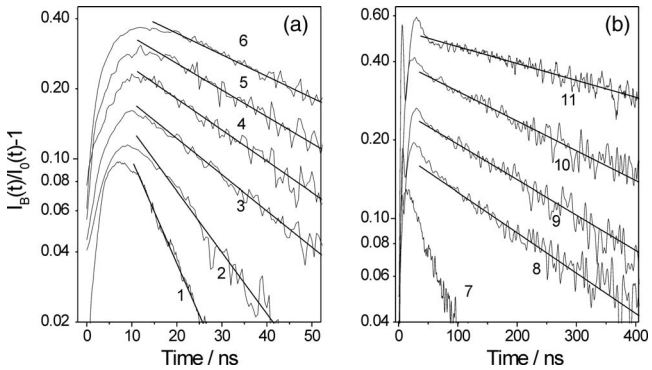

FIG. 4. TR MFE curves for 0.03 M solutions of cH (1), *t*-DEC (2), Et-cH (3), 1,4-Me$_2$-cH (4), *n*Pr-cH (5), cyclohexane-d_{12} (6), Me-cH (7), 1,1-Me$_2$-cH (8), *i*Pr-cH (9), *c*-DEC (10), and *t*Bu-cH (11) in *n*-hexane with the addition of 3 μM *p*TP at 293 K (B = 1 T).

The measured T_1 relaxation times of the studied RCs are listed in Table III. Fig. 5 demonstrates a distinct correlation between the T_1 values and the calculated barrier heights to pseudorotation, E_B. Qualitatively, the relaxation rate increases when the pseudorotation becomes easier.

We studied the dependence of spin-lattice relaxation time on the magnetic field to estimate typical characteristics of the stochastic interaction leading to the paramagnetic relaxation. According to the well-known Redfield theory[1–3]

$$\frac{1}{T_1} = \frac{2(\gamma\Delta)^2 \cdot \tau_c}{1 + (\gamma B \cdot \tau_c)^2}, \tag{3}$$

where Δ is the matrix element of the spin flip transition under perturbation (in magnetic field units), γ is the

TABLE III. Spin-lattice relaxation time T_1 at B= 1 T (293 K, values are averaged over 2–4 experiments) and the parameters of the approximation of the temperature dependences of cycloalkane RC relaxation rate.

Radical cation	T_1 (ns)	E_a (kcal/mol)	A (s^{-1})
Cyclohexane	9	<0.2	1.1×10^8
trans-Decalin	13	0.5	1.8×10^8
Ethylcyclohexane	26	0.9	1.8×10^8
1,4-Dymethylcyclohexane	35	1.8	7×10^8
Propylcyclohexane	46	0.4	4×10^7
Cyclohexane-d_{12}	51	<0.5	$\sim 2 \times 10^7$
Methylcyclohexane	65	2	4.7×10^8
1,1-Dimethylcyclohexane	280	<0.5	$\sim 3.6 \times 10^6$
1,2-Dimethylcyclohexane	300	<0.5	$\sim 3.3 \times 10^6$
iso-Propylcyclohexane	300	<0.5	$\sim 3.3 \times 10^6$
cis-Decalin	400	<0.5	$\sim 2.5 \times 10^6$
tert-Butylcyclohexane	650	<0.5	$\sim 1.5 \times 10^6$

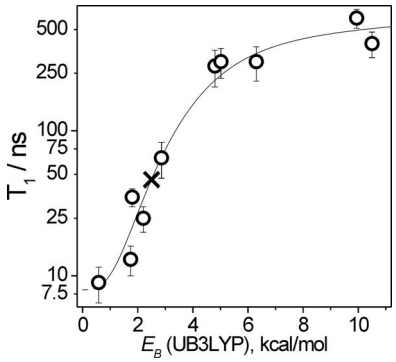

FIG. 5. Correlation between spin-lattice relaxation time, T_1, of cycloalkane RCs (Table III) and the pseudorotation barrier height E_B according to unrestricted B3LYP calculations (Table I). A smooth line is constructed for convenience of perception. The cross indicates probable position of the point for *n*Pr-cH (see the text).

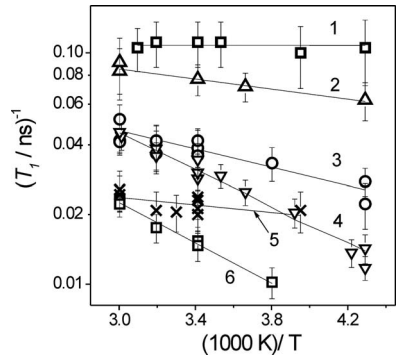

FIG. 7. The rate of spin-lattice relaxation in $cH^{+\bullet}$ (1), *t*-$DEC^{+\bullet}$ (2), Et-$cH^{+\bullet}$ (3), 1,4-Me_2-$cH^{+\bullet}$ (4), *n*Pr-$cH^{+\bullet}$ (5), Me-$cH^{+\bullet}$ (6) at B = 1 T for various temperatures. Straight lines show the exponential approximation by $A \cdot \exp(-E_a/RT)$ functions. The values of A and E_a are listed in Table III.

gyromagnetic ratio for a free electron, B is the magnetic field, and τ_c is the decay time of the autocorrelation function for the stochastic perturbation. Most reliable results were obtained for $cH^{+\bullet}$ and Et-$cH^{+\bullet}$ and are shown in Fig. 6. In both the cases, the estimated correlation time τ_c is about 0.2 ps, and Δ is of the order of 100 mT.

For the further discussion it is important to note that the obtained values should be interpreted as the upper estimate for τ_c and the lower one for Δ. If the perturbation that causes relaxation is only effective a fraction f of time, the factor $f < 1$ should be introduced to the right-hand side of Eq. (3). In this case, for instance, the aforementioned estimate of the perturbation amplitude is of the form $\Delta\sqrt{f} \approx 100$ mT resulting in larger Δ values.

The temperature dependences of the spin-lattice relaxation times of the cycloalkane RCs were measured over the range of 233–333 K. Fig. 7 shows the results obtained for RCs with high relaxation rates. For other RCs, no noticeable temperature dependence of T_1 was found.

As follows from Fig. 7, the temperature dependence of the spin-lattice relaxation rate can be approximated by the Arrhenius equation

$$1/T_1 = A \cdot \exp(-E_a/RT). \tag{4}$$

The activation energy E_a and the pre-exponential factor A obtained for the relaxation rate of these RCs are listed in Table III. Fig. 8 shows the correlation between the activation energy and the calculated barrier height to pseudorotation E_B. These data, except for *n*Pr-cH, demonstrate similarity between E_a and E_B for the RCs with high relaxation rates. Note that the activation energy is typically lower than the barrier height. It appears probable that the E_B values are slightly overestimated due to, particularly, neglect of ZPVE. However, the accuracy of small E_a and E_B values is not sufficient to justify more detailed discussion. The case of *n*Pr-cH will be briefly discussed below.

IV. DISCUSSION

A. Conventional mechanisms of the paramagnetic relaxation

The obtained experimental results additionally support the conclusion[10,11] that the common mechanisms fail to explain the fast paramagnetic relaxation in the RCs studied. Of the most importance is the weak dependence of the spin-lattice relaxation rate on magnetic field strength up to about 1.9 T. The values obtained from these dependences

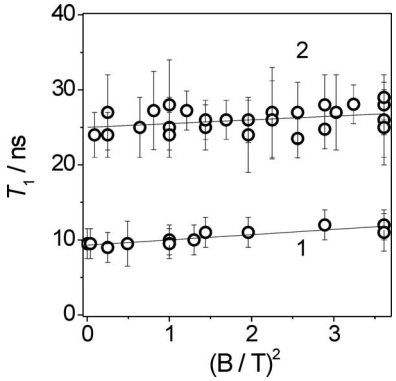

FIG. 6. The dependence of the spin-lattice relaxation time on magnetic induction squared for $cH^{+\bullet}$ (1) and Et-$cH^{+\bullet}$ (2) in *n*-hexane solution at 293 K. Straight lines show the approximation by means of Eq. (3) at $\tau_c \approx 0.16$ ps, $\Delta \approx 106$ mT (1), and $\tau_c \approx 0.3$ ps, $\Delta \approx 50$ mT (2).

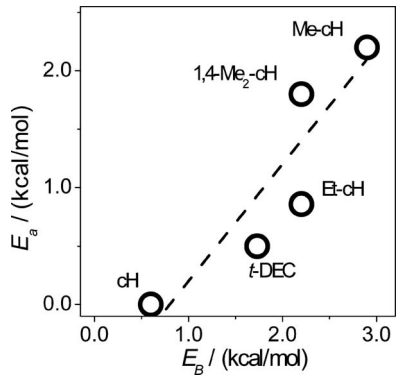

FIG. 8. Correlation between the effective activation energy of the spin-lattice relaxation rate and the pseudorotation barrier height at PES for cycloalkane RCs, with $T_1 < 100$ ns (except for *n*Pr-cH). Straight line is given to guide eyes.

in the framework of the Redfield theory, $\tau_c \sim 0.2$ ps and $\Delta \sim 100$ mT, disagree with the assumption of a substantial contribution of conventional mechanisms to the paramagnetic relaxation. For example, the Δ value is too large to correspond with the HFC modulation due to jumping between stationary structures (Table II) in the radical cations.

The spin-rotational mechanism of paramagnetic relaxation also fails to explain the above estimates of both Δ and τ_c.[43] In this mechanism, the correlation time is the relaxation time of the rotational moment τ_ω, which in a spherical top model equals to[44]

$$\tau_\omega = I/(8\pi r^3 \eta), \tag{5}$$

where I is the inertia moment, r is the radical radius, and η is the dynamic viscosity of a medium. In *n*-hexane ($\eta \approx 0.3$ cP) we get $\tau_\omega \approx 2 \times 10^{-14}$ s for $cH^{+\bullet}$ with estimated $r \approx 0.3$ nm, and $I \approx 4 \cdot 10^{-38}$ g cm^2. A corresponding matrix element can be expressed[43] in terms of the g-tensor component,

$$(\gamma\Delta)^2 \approx (k_B T/3I)[2 \cdot (g_\perp - g_e)^2 + (g_\parallel - g_e)^2], \tag{6}$$

where $k_B T$ is the absolute temperature in energy units. At room temperature, calculations for $cH^{+\bullet}$ ($g_\parallel = 2.0109$, $g_\perp = 2.0046$, Ref. 18) provide $\Delta \approx 27$ mT. For these values, Eq. (3) yields $T_1 \approx 1$ ms that greatly exceeds the experimental value.

Finally, let us consider the mechanism of g-tensor anisotropy modulation by rotational reorientations. In this case, the Δ, a value proportional to the external field, may be of essence in high fields, and the field dependence vanishes at $(B \cdot \tau_c)^2 \gg 1$. The corresponding correlation time is determined by radical reorientation in solution. In the approximation of isotropic diffusion, it is of the form[44]

$$\tau_R = 4\pi r^3 \eta / 3k_B T \tag{7}$$

and the relaxation rate is[1–3]

$$\frac{1}{T_1} = \frac{1}{10} \cdot \left(\frac{\beta B}{\hbar}\right)^2 \cdot \frac{[(g_{ZZ} - \bar{g})^2 + (g_{YY} - \bar{g})^2 + (g_{XX} - \bar{g})^2] \cdot \tau_R}{1 + (\gamma B \tau_R)^2}, \tag{8}$$

where $\bar{g}$ is the averaged g-factor. For $cH^{+\bullet}$ in *n*-hexane, we get $\tau_R \approx 8 \times 10^{-12}$ s. Indeed, the requirement $(B \cdot \tau_R)^2 > 1$ is fulfilled starting from a field of about 1 T. However, the corresponding relaxation time would be $T_1 \sim 10$ ms, much larger than the observed one. Note that RC of cyclohexane exhibits both the largest HFC constants and the g-factor anisotropy as compared to the RCs of other cycloalkanes. Therefore, the above relaxation mechanisms should give even lower relaxation rates for other RCs.

The pseudorotation in the RCs is an intramolecular motion that may have some effect on the above estimates but it does not affect the general conclusion that the conventional mechanisms of relaxation are not effective enough. For example, pseudorotation may accelerate the stochastic modulation of HFCs leaving, however, the matrix element unchanged. Additionally, pseudorotation creates an extra angular momentum of the radical that could increase its spin-lattice relaxation rate via the mechanisms of spin-rotation coupling.[43] The stochastic modulation of the *intramolecular* pseudorotation could precede on a time scale larger as compared to τ_ω, which relates to intermolecular interactions. However the corresponding contribution to the relaxation rate is probably insignificant since the value of the inertia moment for the pseudorotation is very low (see its estimated value below).

B. Qualitative interrelations between the spin-lattice relaxation, the degeneracy of vibronic levels and pseudorotation

It is well known that for particles with the non-zero orbital momentum the observation of paramagnetic resonance in the condensed phase becomes possible, partially, due to the phenomenon referred to as the "freezing of the orbital moment".[3] It denotes a dramatic decrease in the spin-orbital coupling (SOC) in radicals due to removing the orbital degeneracy since the interactions of unpaired electron with neighboring atoms are of low symmetry. In a Jahn-Teller active radical, the intermolecular interactions cause a PES distortion that tends to stabilize a particular geometry of the radical along with decreasing effects of spin-orbital coupling. Nevertheless, a hypothesis has been repeatedly suggested[45,46] that in these radicals the degeneracy of vibronic states can be restored. The degeneracy has been considered to lead to the relatively strong SOC, which is responsible for the fast paramagnetic relaxation in highly symmetric radicals.

Some evidence of such a behavior is given by EPR experiments on spin-lattice relaxation of paramagnetic species with nearly degenerate ground state in solid phase under stress.[47,48] It has been found that increasing stresses decelerate the spin-lattice relaxation. This can be assigned to the fact that the applied stress, i.e., the external asymmetric potential, increases the splitting of the initially degenerate states and, thus, decreases both the spin-orbital coupling and the relaxation rate.

In solutions, the interaction with a solvent is characterized by a low symmetry, and it removes the degeneracy of vibronic states of symmetric radicals like cyclohexane RC, which has a degenerate ground state in vacuum. Unlike the solid phase, in liquids, the intermolecular interaction is a stochastic process due to molecular motions and, surely, it changes the relative positions of the vibronic states. Therefore, the vibronic degeneracy is expected to be restored for a moment with a characteristic period of the order of the time between intermolecular collisions or rotations. The introduction of substituents to the cyclohexane ring causes a permanent splitting of vibronic states. It is likely that if the value of the permanent splitting of particular vibronic states exceeds those caused by a typical interaction with the solvent then the degeneracy of these states is hardly to be restored.

Since no information on actual vibronic state energies in RCs studied is available we have complemented the above qualitative picture by an additional assumption: typically (not necessary), the vibronic states are splitted by a *nonsymmetric* substitution if the energies of these states are below the barrier height to pseudorotation in these RCs. Besides, it is very probable that the splitting increases with the barrier height. This assumption finds a partial support in the experimental

results. Indeed, the shortest relaxation time is observed in $cH^{+\bullet}$, where the degeneracy is evidently restored with the highest probability. The increase in the barrier height to pseudorotation in RCs correlate as suggested with the decrease in the spin-lattice relaxation rate (Fig. 5). It can be interpreted as a result of an increasing splitting of the vibronic levels that leads to a decrease in the probability of the degeneracy recovering. For the radical cations of *c*-DEC and *t*Bu-cH with the highest barriers, the relaxation time approaches the values typical of organic free radicals indicating that in these cases, the specific relaxation mechanism becomes negligible and the relaxation is determined by the conventional ones.

On the other hand, the above hypothesis allows one to speculate on the correlation between the relaxation rate and the possibility of the pseudorotation in the radical. The results demonstrated in Figs. 5 and 8 can be considered as evidence that the effective coupling of the unpaired electron spin with other degrees of freedom and, thus, the fast spin-lattice relaxation can arise from the excitation of "free" pseudorotation in the radical. This view is reasonable since actually free pseudorotation with a perceptible contribution to the angular moment takes place when the vibronic states are degenerate. It appears probable that vibronic states, whose energy is above the barrier to pseudorotation, E_B, are nearly degenerate since the effect of the distorted PES bottom should decrease with the increase in this energy. Thus, the excitation to above the barrier is equivalent to the excitation to a quasi-degenerate vibronic state where the degeneracy can be restored with an appreciable probability.

C. Spin-orbital coupling (SOC) in cyclohexane radical cation

For the mechanism discussed, it is important to know how strong SOC is when the degeneracy is restored in the radical ions under consideration. It is easy to estimate the maximum possible magnitude of SOC. This could be reached at the conical intersection point where the electronic state is doubly degenerate. Our calculations (CASSCF(5,5)/6-311G*) have shown that the values of SOC constant, λ, at this point for $cH^{+\bullet}$, Me-$cH^{+\bullet}$, and Et-$cH^{+\bullet}$ amount to 15.8 cm^{-1}, 13.1 cm^{-1}, and 13.4 cm^{-1}, respectively. Such high values originate from the fact that the molecular orbitals of the aliphatic RCs include the carbon sp^3 orbitals, the SOC constant being $\approx$28 cm^{-1} for *p*-orbital of carbon atom.[49]

Removing $cH^{+\bullet}$ from the conical intersection point to the bottom of pseudorotation trough conserves the degeneracy of the vibronic ground state but leads to a decrease in the SOC constant.[50] It is possible to estimate effective SOC constant λ' in the ground vibronic state of $cH^{+\bullet}$ using the results of Ref. 51. In the cited work it was shown that at linear vibronic interactions the Ham's factor $p = \lambda'/\lambda$ may be approximated by the formula

$$p = \exp\left[-1.974 \cdot \left(\frac{\Delta E_{JT}}{\hbar\omega}\right)^{0.761}\right], \qquad (9)$$

where ΔE_{JT} is the radical stabilization energy in respect to the conical intersection point determined by the interaction with a given vibration, and ω is the frequency of this vibration. Note that there are several vibrational modes involved in the vibronic interaction in $cH^{+\bullet}$. In Ref. 52 studying the Rydberg states of cH molecules, six E_g modes in the frequency range 405–1280 cm^{-1} with the corresponding ΔE_{JT} values for each mode over the range 110–1470 cm^{-1} were referred to as Jahn-Teller active modes. The data obtained for the highly excited molecule state may also be assigned to the RC, which is a residue of the molecule. Assuming the contributions of various vibrational modes to Ham's factor to be additive by analogy with the $(T\times e)$ Jahn-Teller problem,[50] from Eq. (9) we get $p \sim 5 \times 10^{-3}$ and hence, $\lambda' \sim 0.1$ cm^{-1}.

For $cH^{+\bullet}$, one more approach is possible to estimate λ'. It appears likely that upon pseudorotation, the averaged electron motion relative to the carbon nuclei in the radical cation is similar to that in the free carbon atom. However, the frequency of this motion should be approximated by the pseudorotation frequency ω_p, which is much lower as compared to the characteristic frequency of electron motion in the carbon atom, ω_e. We assume then that $\lambda' \sim \lambda(\omega_p/\omega_e)$. In Ref. 52, the estimate $\omega_p \approx 150$ cm^{-1} was obtained for the ground vibronic state from the analysis of spectroscopic data on the Rydberg state of the cH molecule. We have also estimated ω_p for $cH^{+\bullet}$ using a classical pseudorotation model proposed in Ref. 53. To this end, we have calculated the pseudorotation inertia moment $I_j = \mu r_0^2$, where μ is a reduced mass for pseudorotation, and r_0 is the amplitude of nucleus motion upon pseudorotation.[19,53] With the calculated $I_j \approx 3 \times 10^{-41}$ g cm^2 the pseudorotation frequency was estimated as $\omega_p \approx (kT/I_j)^{1/2} \approx 1000$ cm^{-1}. It is worth noting that this estimate takes into account the contribution of all thermally excited vibronic states and the substantial difference in the two estimates is of no surprise. From these estimates, assuming that $\omega_e \approx 50\,000$ cm^{-1} and $\lambda \approx 28$ cm^{-1}, we estimate λ' to be within the range of 0.09–0.6 cm^{-1}.

Considering the above evaluations, it is likely to assume that a reasonable estimate of the effective SOC constant in the ground state of $cH^{+\bullet}$ is $\lambda' \sim 0.1$ cm^{-1}. In magnetic field units, it is equivalent to 100 mT, i.e., to the estimated matrix element Δ of the relaxation transition derived from the field dependence of the relaxation times of $cH^{+\bullet}$ and Et-$cH^{+\bullet}$.

Note that the above consideration gives the upper estimate for the scale of SOC in $cH^{+\bullet}$ Even for isolated radical cations, the factor p and the λ' value may be smaller due to quadratic vibronic interactions.[54] The quadratic effect keeps the degeneracy of the ground vibronic state but gives rise to the barrier to pseudorotation.[19] By analogy with the $(T\times e)$ Jahn-Teller problem,[50] it can be interpreted as the result of a decrease in the overlap of the vibrational nuclear wave functions of various vibronic states upon PES distortion[50] and a corresponding decrease in the Ham's factor p. For $cH^{+\bullet}$, the calculated distortions of the PES profile, which may be assigned to quadratic corrections (see Fig. 1), are not large ($<k_BT$), and in the present discussion their effect is neglected.

D. Spin relaxation due to stochastic crossing of vibronic levels

For further discussion, let us remember the energy scale of various interactions in a Jahn-Teller active radical ion by an example of $cH^{+\bullet}$. The magnitude of the vibronic levels splitting induced by the relevant interactions decreases in the following order: the vibronic interaction in the RC ($\sim 10^4$ cm^{-1}), the effect of a solvent ($\sim 10^2$ cm^{-1}, see the discussion of this effect below), the Zeeman interaction (~ 1 cm^{-1} at B = 1 T), and the spin-orbital coupling (~ 0.1 cm^{-1}). In this case, the interaction with the solvent, which is independent of electron spin, varies stochastically and results in crossing of the Zeeman sublevels of the different vibronic states.

In a simple McConnel's model,[46] pulsed SOC in a Jahn-Teller active radical efficiently mixes the different Zeeman sublevels when vibronic levels become degenerate within the accuracy of λ'. This is a very transient event since the estimated $\lambda' = 0.1$ cm^{-1} is much smaller than the solvent induced splitting $\sim 10^2$ cm^{-1}. As a consequence, the probability of spin flip during the degeneracy recovering is very small, and the model[46] of "pulsed" SOC is inadequate to explain the fast relaxation rates.

Instead, we should consider a more detailed model of spin evolution in the course of *vibronic level crossing*, which is schematically shown in Fig. 9. We shall assume that the vibronic levels move smoothly enough due to the solvent effect and the vibrational relaxation time is long enough. Let us introduce the characteristic magnitude of the splitting between the vibronic levels as caused by interactions with solvent, δ, and typical time between the changes of the relative positions of the levels, τ. Due to interference effects in the four-level system (see, e.g., Ref. 55), the level crossing can result in a non-trivial redistribution of the spin level populations that, in particular, can depend on magnetic field and τ. However, in this work we estimate only the scale of feasible effects.

To do this, we use the known Landau-Zener formula[56] for the probability P of the non-adiabatic transition with a single crossing of a pair of levels (at $P \ll 1$),

$$P = \frac{2\pi V^2}{\hbar \upsilon F}. \tag{10}$$

In this case, $V \sim \lambda'$ is the transition matrix element, which is assumed constant, υ denotes the rate of the change in the parameter describing the approach to the intersection point, and F is the derivative of the splitting value with respect to this parameter. As a crude estimation, we get $\upsilon F \sim 2\delta/\tau$. Thus, the spin-lattice relaxation time can be estimated as

$$T_1 \sim \frac{\tau}{P} \sim \frac{\hbar\delta}{\pi\lambda'^2}. \tag{11}$$

This equation, with the experimentally observed value $T_1 = 10$ ns and $\lambda' = 0.1$ cm^{-1}, gives $\delta \sim 10^2$ cm^{-1}.

In order to support the relaxation model, it is important to compare this value of δ with a splitting of degenerate vibronic states observed in condensed media with other experimental techniques. This comparison can be performed using the results of extensive optical and Zeeman studies of metalloporphyrins. As an example, according to the data reported in Refs. 57–59, in normal alkane crystals at 4.2 K the vibronic state splitting induced by the crystal field in various metalloporphins ranged from 40 to 110 cm^{-1} that gives a scale of the expected solvent effect. Besides, analysis of optical and magnetic circular dichroism spectra of metallocoproporphyrins performed by Sutherland *et al.*[60] has shown that vibronic states in these compounds in organic solvents are splitted by 50–100 cm^{-1}. Therefore, the similarity of the estimated value of δ and the splittings of degenerate vibronic states observed in organic solvents supports the suggested relaxation model.

It is interesting to rearrange Eq. (11) to the form similar to Eq. (3) obtained within the Redfield theory of spin relaxation in the limit of very short correlation times. To this end, along with Ref. 61 we introduce the transition time t_{tr} as the time for which the transition probability rises to the region of its asymptotic value and use the expression obtained in the cited work for a case of constant matrix element of the transition between diabatic levels at $P \ll 1$

$$\tau_{tr} = \sqrt{\frac{2\pi\hbar}{\upsilon F}}. \tag{12}$$

Equations (10)–(12) are used to express the spin-lattice relaxation rate as

$$\frac{1}{T_1} \sim 2\frac{\lambda'^2}{2\hbar^2}\tau_{tr}\frac{\tau_{tr}}{\tau}. \tag{13}$$

Equation (13) qualitatively coincides with Eq. (3) when we consider λ' as the perturbation amplitude and t_{tr} as the correlation time. The fraction of time during which the system remains in the region where the transition rate becomes of essence amounts to $f = \tau_{tr}/\tau$. In the case under consideration, at $T_1 \sim 10$ ns and $\lambda' \sim 0.1$ cm^{-1}, $\tau_{tr}{}^2/\tau \sim 0.2$ ps. The discussed model of the relaxation mechanism implies that $\tau_{tr}/\tau \leq 1$ to provide the decay of possible coherence effects at the repetitive level crossing. Additionally, it gives the estimate $\tau_{tr} \geq 0.2$ ps, which, at $\tau_{tr}/\tau \approx 1$, agrees with the above estimation $\tau_c \sim 0.2$ ps. Unfortunately, the simplest consideration resulting in Eq. (11) does not allow detailed discussing both effect of external magnetic field and the relationship between τ_{tr} and τ_c.

In this case, we have to admit that the estimation of the relaxation rate made with Eq. (11) corresponds to $f = \tau_{tr}/\tau \sim 1$ in the Redfield theory. This is in a full disagreement with a model[46] of "pulsed" switching on the SOC where $f \sim \lambda'/\delta \sim 10^{-3}$ and implies that spin flip transitions efficiently occur far outside the crossing point.

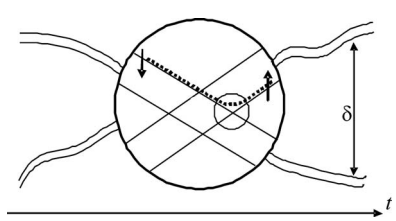

FIG. 9. A scheme of the crossing of the Zeeman sublevels of vibronic states. The dashed line indicates the feasible way of system evolution with electron spin flip. δ is the characteristic value of the splitting of vibronic states due to the interaction with the solvent.

The above consideration should be completed by the estimation of the effect of transitions between different vibronic levels as caused by the vibrational relaxation in the radical. If such transitions were much faster as compared to the interchange of the relative positions of the nearly degenerate states by the external potential then the above model of the spin transitions would make no sense, and the rate of paramagnetic relaxation due to the "vibronic level crossing" mechanism would be very probable to decrease. To this point, it is instructive to mention the results reported in Ref. 62, where the pseudorotation correlation time for cyclopentane in liquid state was estimated to be 0.1 ps. If the coherency lifetimes in the low-lying vibronic states in cyclohexane radical cation are not shorter than this value then estimations made in this section are valid.

Within the frameworks of our hypothesis, it appears likely that the states that are degenerate in $cH^{+\bullet}$ are nearly degenerate in R-$cH^{+\bullet}$ at energies close to and higher than the height of the barrier to pseudorotation. Neglecting the dependence of the Ham's factor on the quantum number for the low-lying vibronic states one can expect the pre-exponential factor in Eq. (4) to be on the same order of magnitude as that for the relaxation rate in the generic case, $cH^{+\bullet}$. The data of Table III qualitatively confirm this assumption for the RCs with $T_1 < 100$ ns. Note that within the "vibronic level crossing" mechanism formulated above, we may consider the radicals without referring to their symmetry properties. Actually, the series includes the RC of the low-symmetric *trans*-decalin. On the other hand, there are exceptional cases of propylcyclohexane and deuterated cyclohexane that will be discussed below.

E. Particular features of some RCs

The discussed model can be questioned using the results obtained for particular radical cations, namely cH-$d_{12}{}^{+\bullet}$, *n*Pr-$cH^{+\bullet}$, and 1,3-dimethyladamantane$^{+\bullet}$, which was studied previously.[11] The relaxation rate is high enough in these cases, and there is no doubt that the mechanism of spin-lattice relaxation has the same origin as in the case of $cH^{+\bullet}$. At the same time, these radical cations exhibit some peculiarities when comparing with other radicals under study.

1. Cyclohexane-d_{12}

As shown in Table III, the deuteration of $cH^{+\bullet}$ results in the slowing down of the paramagnetic relaxation by a factor of 5. This deuteration effect appears to be unexpected for two reasons. First, this contradicts the case of benzene-d_6 radical anion in which the deuteration fails to retard the paramagnetic relaxation.[63] Second, according to Ref. 52, in the Rydberg state of cyclohexane molecule, the values of vibronic interactions in both protonated and deuterated cyclohexane are almost the same, which raises the question on the validity of the relaxation model.

We have assumed that the deuteration effect is caused by the difference in the vibrational spectra in the region of the Jahn-Teller active vibrational modes, which causes an increase in the vibrational relaxation rate in the deuterated cyclohexane. According to Ref. 52, the wave number range of the Jahn-Teller active vibrations in the Rydberg $3s^1E_g$ state, upon deuteration changes from 426–1443 cm^{-1} to 373–1212 cm^{-1}. On the other hand, it is known[64] that in the vibrational spectrum of cH molecule, the deuteration substantially changes the position of the lines related to the vibrations in the CH_2 group. The wave numbers for the v_{14} (A_{2u}) and v_{27} (E_u) vibrations in the *c*-C_6H_{12} molecule are both equal to 1456 cm^{-1} while upon transition to *c*-C_6D_{12}, these wave numbers decrease to 1092 cm^{-1} and 1076 cm^{-1}, respectively. Therefore, they fall within the range of the Jahn-Teller active vibrations. The same is very probable to be valid for radical cations since the vibrational spectrum of cyclohexane molecule is very similar to that of its Rydberg state, where the molecular residue is just the radical cation. Thus, the deuteration is probable to cause an increase in the vibrational state density in the region of the Jahn-Teller active vibrations in cyclohexane RC that could be a reason of a substantial acceleration of the vibrational relaxation accompanied by a slowing of the spin-lattice relaxation down.

In contrast to cyclohexane, there is no such mixing in the vibrational spectrum in the benzene molecule. For the benzene radical anion, Jahn-Teller active vibrations are of the E_{2g} type (see, e.g., Ref. 65). In the benzene molecule, the vibrations of this type range from 606 to 3047 cm^{-1} in C_6H_6 and from 577 to 2265 cm^{-1} in C_6D_6. No additional modes appear within the range upon deuteration.

2. Propylcyclohexane

According to the BHHLYP calculations, the barrier height to pseudorotation for *n*Pr-$cH^{+\bullet}$ occupies an intermediate position among the studied RCs. From this point, the position in the ascending part of the curve in Fig. 5 is quite expected for this particle. However, the temperature dependence of the relaxation rate in this RC is too weak. A possible explanation could be that some vibronic states with the energies lower than the pseudorotation barrier are nearly degenerate with the splitting less than $\sim$100 cm^{-1}. According to the above assumption, high activation energy is not necessary in this case.

Alternatively, this could be an effect of transitions between different PES sheets accompanied by the rotation of the propyl fragment. However, quantum-chemical calculations have demonstrated that such possibility is likely of no significance since barriers for such transitions are similar to or larger than the barriers to pseudorotation, which in turn are only slightly dependent of the particular PES sheet.

3. 1,3-Dimethyladamantane

Although this work discusses only the radical cations of cyclohexane derivatives, it is likely that the same mechanism is responsible for the fast spin-lattice relaxation in RCs of adamantane and its derivatives.[11] As shown in the cited work, there is no significant difference between the relaxation rate in the adamantane and 1,3-dimethyladamantane RCs. One

would expect that introducing two methyl groups increases the pseudorotation barrier, whose value correlates with relaxation rate. However, adamantane RC is a system with triple degeneracy, where a quasi-one-dimensional pseudorotation trough transforms into the quasi-two-dimensional one (see, e.g., Ref. 16). It could be assumed then that the introduction of two methyl groups increases the pseudorotation barrier only for a part of feasible trajectories of a motion over the pseudorotation hypersurface while the unhindered pseudorotation remains possible for other quasi-one-dimensional trajectories. In other words, to remove completely the degeneracy in triply degenerate systems, a stronger non-symmetric perturbation is required as compared to double degenerate ones.

4. Linear radicals

The above consideration can be applied to linear radicals where the degeneracy of orbital states is not removed due to Jahn-Teller effect. In solution, these states are also to be affected by intermolecular interactions, which remove the degeneracy. Stochastic changes in the relative positions of the initially degenerate orbital states should result in the spin-lattice relaxation in the radical. SOC constant in such radicals[49,66] may be comparable with the expected magnitude of the interaction with solvent. Thus, the corresponding spin relaxation transitions should proceed very effectively. However, this contribution to the paramagnetic relaxation rate seems to be difficult to distinguish against the contributions made by the ordinary mechanisms, where spin-orbit interaction is operative, like the g-tensor anisotropy modulation or spin-rotation interaction.

V. CONCLUSIONS

The method of time-resolved magnetic field effect was applied to measure the rates of spin-lattice relaxation in the radical cations of the cycloalkane series in solution at different temperatures and magnetic field strengths. Combining the experimental results with quantum-chemical calculations (DFT) of the adiabatic surfaces of the potential energy of the radical cations, an evident correlation between the relaxation rate and the calculated barrier height, E_B, to the pseudorotation in these RCs has been found. Besides, for the majority of the radical cations with high relaxation rates, the apparent activation energies for the spin-lattice relaxation rate are similar to the calculated values of E_B.

The hypothesis on the mechanism of the unusually effective spin-lattice relaxation in the cycloalkane RCs has been proposed. It is assumed, first, that the vibronic states degeneracy, which is specific for Jahn-Teller active systems, is approximately kept for the states with the energy slightly above or close to the barrier to pseudorotation without any relation to the symmetry properties. Second, the relaxation spin transitions are suggested to be caused by the crossings of the nearly degenerate vibronic states that take place due to fluctuations of the interaction between the radical and the solvent. The above model may be also applied to other radicals with degenerate or nearly degenerate (<100 cm^{-1}) ground or low-lying states such as the linear radicals, radicals with the threefold degeneracy, etc. It looks likely that this paramagnetic relaxation mechanism can be quenched by fast vibrational relaxation in radicals.

ACKNOWLEDGMENTS

This work was financially supported by the Council for Grants of the President of the Russian Federation for State Support of Leading Scientific Schools (Grant No. NSh–2272.2012.3) and by the Division of Chemistry and Materials Science, RAS (Grant No. 5.1.6, 2010-2012).

[1] A. Carrington and A. D. McLachlan, *Introduction To Magnetic Resonance With Application To Chemistry And Chemical Physics* (Harper&Row, NewYork, 1967).
[2] J. E. Wertz and J. R. Bolton, *Electron Spin Resonance: Elementary Theory and Practical Applications* (McGraw-Hill, NewYork, 1972).
[3] C. P. Slichter, *Principles of Magnetic Resonance* (Springer-Verlag, Berlin, 1990).
[4] D. M. Bartels, R. G. Lawler, and A. D. Trifunac, J. Chem. Phys. **83**, 2686 (1985).
[5] M. G. Townsend and S. I. Weissman, J. Chem. Phys. **32**, 309 (1960).
[6] M. R. Das, S. B. Wagner, and J. H. Freed, J. Chem. Phys. **52**, 5404 (1970).
[7] A. J. Schell-Sorokin, F. Mehran, G. R. Eaton, S. S. Eaton, A. Viehbeck, T. R. O'Toole, and C. A. Brown, Chem. Phys. Lett. **195**, 225 (1992).
[8] M. Brustolon, A. Zoleo, G. Agostini, and M. Maggini, J. Phys. Chem. A **102**, 6331 (1998).
[9] A. Pénucaud, A. Peréz-Benítez, R. Escudero, and C. Coulon, Solid State Commun. **96**, 147 (1995).
[10] V. I. Borovkov and Yu. N. Molin, Phys. Chem. Chem. Phys. **6**, 2119 (2004).
[11] V. I. Borovkov and Yu. N. Molin, Chem. Phys. Lett. **398**, 422 (2004).
[12] J. H. Freed, J. Chem. Phys. **49**, 376 (1968).
[13] S. C. Benjamin, A. Ardavan, G. A. D. Briggs, D. A. Britz, D. Gunlycke, J. Jefferson, M. A. G. Jones, D. F. Leigh, B. W. Lovett, A. N. Khlobystov, S. A. Lyon, J. J. L. Morton, K. Porfyrakis, M. R. Sambrook, and A. M. Tyryshkin, J. Phys.: Condens. Matter **18**, S867 (2006).
[14] M. Zaka, Y. Ito, H. Wang, W. Yan, A. Robertson, Y. A. Wu, M. H. Rümmeli, D. Staunton, T. Hashimoto, J. J. L. Morton, A. Ardavan, G. A. D. Briggs, and J. H. Warner, ACS Nano **4**, 7708 (2010).
[15] M. Shiraishi and T. Ikoma, Physica E (Amsterdam) **43**, 1295 (2011).
[16] I. Bersuker, Chem. Rev. **101**, 1067 (2001).
[17] I. B. Bersuker and V. Z. Polinger, *Vibronic Interactions in Molecules and Crystals* (Springer-Verlag, Berlin, 1989).
[18] M. Iwasaki, K. Toryama, and K. Nunome, Faraday Discuss. Chem. Soc. **78**, 19 (1984).
[19] A. F. Sax, Chem. Phys. **349**, 9 (2008).
[20] P. Wang, M. Shiotani, and S. Lunell, Chem. Phys. Lett. **292**, 110 (1998).
[21] R. M. Kadam, Y. Itagaki, N. P. Benetis, A. Lund, R. Erickson, M. Huber, and W. Hilczer, Phys. Chem. Chem. Phys. **1**, 4967 (1999).
[22] V. I. Feldman, F. F. Sukhov, and A. Yu. Orlov, Chem. Phys. Lett. **300**, 713 (1999).
[23] V. I. Borovkov, I. V. Beregovaya, L. N. Shchegoleva, V. A. Bagryanskii, and Yu. N. Molin, Dokl. Phys. Chem. **426**, Part 2, 108 (2009).
[24] I. V. Beregovaya and L. N. Shchegoleva, Int. J. Quant. Chem. **88**, 481 (2002).
[25] V. P. Vysotsky, G. E. Salnikov, and L. N. Shchegoleva, Int. J. Quant. Chem. **100**, 469 (2004).
[26] M. M. Barlukova, I. V. Beregovaya, V. P. Vysotsky, L. N. Shchegoleva, V. A. Bagryansky, and Yu. N. Molin, J. Phys. Chem. A **109**, 4404 (2005).
[27] I. V. Beregovaya, L. N. Shchegoleva, and V. I. Borovkov, J. Phys. Chem. A **113**, 1555 (2009).
[28] V. A. Bagryansky, V. I. Borovkov, and Yu. N. Molin, Russ. Chem. Rev. **76**, 493 (2007).
[29] V. V. Lozovoy, S. V. Anishchik, N. N. Medvedev, O. A. Anisimov, and Yu. N. Molin, Chem. Phys. Lett. **167**, 122 (1990).
[30] S. V. Anishchik, V. M. Grigoryants, I. V. Shebolaev, Y. D. Chernousov, O. A. Anisimov, and Y. N. Molin, Prib. Tekh. Eksp. (Russ.) **4**, 74 (1989).
[31] A. D. Becke, J. Chem. Phys. **98**, 5648 (1993); C. T. Lee, W. T. Yang, and R. G. Parr, Phys. Rev. B **37**, 785 (1988).
[32] A. D. Becke, J. Chem. Phys. **98**, 1372 (1993).

[33]M. W. Schmidt, K. K. Baldridge, J. A. Boatz, S. T. Elbert, M. S. Gordon, J. H. Jensen, S. Koseki, N. Matsunaga, K. A. Nguyen, S. J. Su, T. L. Windus, M. Dupuis, and J. A. Montgomery, J. Comput. Chem. **14**, 1347 (1993).
[34]M. Shiotani, M. Lindgren, N. Ohta, and T. Ichikawa, J. Chem. Soc. Perkin Trans. **2**, 711 (1991).
[35]K. Toriyama, K. Matsuura, and K. Nunome, Chem. Phys. Lett. **169**, 311 (1990).
[36]L. Sjoqvist, M. Lindgren, A. Lund, and M. Shiotani, J. Chem. Soc. Faraday Trans. **86**, 3377 (1990).
[37]M. Lindgren, M. Shiotani, N. Ohta, T. Ichikawa, and L. Sjoqvist, Chem. Phys. Lett. **161**, 127 (1989).
[38]S. Lunell, M. B. Huang, O. Claesson, and A. Lund, J. Chem. Phys. **82**, 5121 (1985).
[39]D. W. Werst, M. G. Bakker, and A. D. Trifunac, J. Am. Chem. Soc. **112**, 40 (1990).
[40]M. J. Frisch, G. W. Trucks, H. B. Schlegel *et al.*, GAUSSIAN 94, Revision D.4, Gaussian, Inc., Pittsburgh, PA, 1995.
[41]Y.-J. Liu and M. B. Huang, J. Mol. Struct.: THEOCHEM. **536**, 133 (2001).
[42]J. Tirado-Rives and W. L. Jorgensen, J. Chem. Theory Comput. **4**, 297 (2008).
[43]P. W. Atkins and D. Kivelson, J. Chem. Phys. **44**, 169 (1966).
[44]P. S. Hubbard, Phys. Rev. **131**, 1155 (1963).
[45]D. Kivelson, J. Chem. Phys. **45**, 751 (1966).
[46]H. M. McConnell, J. Chem. Phys. **34**, 13 (1961).
[47]K. Toriyama and M. Okazaki, Acta Chem. Scand. **51**, 167 (1997).
[48]D. C. Krupka and R. H. Silsbee, Phys. Rev. **152**, 816 (1966).
[49]I. V. Khudyakov, Y. A. Serebrennikov, and N. J. Turro, Chem. Rev. **93**, 537 (1993).
[50]F. S. Ham, Phys. Rev. **138**, 1727 (1965).
[51]F. S. Ham, Phys. Rev. **166**, 307 (1968).
[52]R. L. Whetten and E. R. Grant, J. Chem. Phys. **80**, 1711 (1984).
[53]V. V. Diky, N. V. Martsinovich, and G. J. Kabo, J. Phys. Chem. A **105**, 4969 (2001).
[54]N. Sakamoto, Phys. Rev. B **31**, 785 (1985).
[55]T. Usuki, Phys. Rev. B **56**, 13360 (1997).
[56]L. D. Landau and L. M. Lifshitz, *Quantum Mechanics: Non-Relativistic Theory*, 5th ed. (Fizmatlit, Moscow, 2001), Vol. 3 (in Russian).
[57]G. W. Canters, J. A. Kooter, N. van Dijk, and J. H. van der Waals, J. Lumin. **18/19**, 196 (1979).
[58]G. W. Canters, J. van Egmond, T. J. Schaafsma, and J. H. van der Waals, Mol. Phys. **24**, 1203 (1972).
[59]N. van Dijk, M. Noort, S. Voelker, G. W. Canters, and J. H. van der Waals, Chem. Phys. Lett. **71**, 415 (1980).
[60]J. C. Sutherland, D. Axelrod, and M. P. Klein, J. Chem. Phys. **54**, 2888 (1971).
[61]N. V. Vitanov, Phys. Rev. A **59**, 988 (1999).
[62]R. A. MacPhail and J. E. Variyar, Chem. Phys. Lett. **161**, 239 (1989).
[63]R. G. Lawler and G. K. Fraenkel, J. Chem. Phys. **49**, 1126 (1968).
[64]L. M. Sverdlov, M. A. Kovner, and E. P. Krainov, *Vibrational Spectra of Multiatomic Molecules* (Nauka, Moscow, 1970) (in Russian).
[65]K. Tokunaga, T. Sato, and K. Tanaka, J. Chem. Phys. **124**, 154303 (2006).
[66]G. Herzberg and J. W. T. Spinks, *Molecular Spectra and Molecular Structure. I. Spectra of Diatomic Molecules*, 2nd ed. (D. Van Nostrand, Princeton, 1950).